inferred, for the reasons set forth by Keener and Chapman,[1] that vortex-asymmetry onset is due principally to a hydrodynamic instability phenomenon rather than to the occurrence of laterally asymmetric viscous separation. The foregoing considerations assume that vortex bursting has not occurred forward of the trailing edge.

Experimental Verification

Experimental representations for the onset angle of attack α_{va} for vortex asymmetry as a function of semiapex angle δ_n are shown in Fig. 2 for flat delta wings and circular cones. The experimental data points have been represented by faired straight lines for the sake of clarity. The data for the delta wings are taken from Refs. 3-6, whereas those for the circular cones are taken from Refs. 7-10. The straight-line slope for the cone data differs slightly from that used by Keener and Chapman[1] because of the use of a different onset criterion. Details regarding the interpretation of the experimental data may be obtained by contacting the author.

The consequence of application of the similarity parameter K to experimental circular-cone vortex-asymmetry data for lateral separation angles ranging from laminar separation ($\theta_s = 30$ deg) to turbulent separation ($\theta_s = 55$ deg) is shown by the crosshatched region in Fig. 2. It is seen here that the application of the similarity parameter brings the cone data into general agreement with the delta wing data.

Concluding Remarks

The foregoing analysis is not intended to be a definitive treatment of the subject of vortex-asymmetry onset, but rather to provide some insight into a complicated phenomenon by means of a simple analytic model. If one accepts the approximations involved, the analysis favors attributing vortex-asymmetry onset for delta wings and circular cones to a hydrodynamic instability phenomenon. This does not preclude the possibility of a viscous asymmetric separation cause and effect, but such a determination requires a more rigorous analysis than the one presented herein.

References

[1] Keener, E. R. and Chapman, G. T., "Similarity in Vortex Asymmetries over Slender Bodies and Wings," *AIAA Journal*, Vol. 15, Sept. 1977, pp. 1370-1372.

[2] Ericsson, L. E. and Reding, J. P., "Steady and Unsteady Vortex-Induced Asymmetric Loads on Slender Vehicles," *Journal of Spacecraft and Rockets*, Vol. 18, March-April 1981, pp. 97-109.

[3] Shanks, R. E., "Low-Subsonic Measurements of Static and Dynamic Stability Derivatives of Six Flat-Plate Wings Having Leading-Edge Sweep Angles of 70° to 84°," NASA TND-1822, 1963.

[4] Bird, J. D., "Tuft-Grid Surveys at Low Speeds for Delta Wings," NASA TND-5045, Feb. 1969.

[5] Polhamus, E. C., "Predictions of Vortex-Lift Characteristics by a Leading-Edge Suction Analogy," *Journal of Aircraft*, Vol. 8, April 1971, pp. 193-199.

[6] Erickson, G. E., "Vortex Flow Correlation," Air Force Systems Command, Tech. Rept. AFWAL-TR-80-3143, Jan. 1981.

[7] Coe, P. L. Jr., Chambers, J. R., and Letko, W., "Asymmetric Lateral-Directional Characteristics of Pointed Bodies of Revolution at High Angles of Attack," NASA TND-7095, 1973.

[8] Orlik-Rückemann, K. J., LaBerge, J. G., and Iyengar, S., "Half- and Full-Model Experiments on Slender Cones at Angles of Attack," *Journal of Spacecraft and Rockets*, Vol. 10, Sept. 1973, pp. 575-580.

[9] Keener, E. R., Chapman, G. T., Cohen, L., and Taleghani, J., "Side Forces on Forebodies at High Angles of Attack and Mach Numbers from 0.1 to 0.7: Two Tangent Ogives, Paraboloid and Cone," NASA TM X-3438, 1976.

[10] Peake, D. J. and Owen, F. K., "Control of Forebody Three-Dimensional Flow Separation," Paper 17 in AGARD-CP-262, Sept. 1979.

AIAA 82-4097

Axisymmetric Inviscid Swirling Flows Produced by Bellmouth and Centerbody

Yoshiaki Nakamura,* Toshio Hama† and Michiru Yasuhara‡

Nagoya University, Nagoya, Japan

Introduction

MANY researchers, such as Harvey,[1] Sarpkaya,[2-4] and Faler and Leibovich,[5,6] have used similar apparatus to conduct experiments on vortex breakdown in a pipe. The equipment to generate the swirling flows consists of bellmouth and centerbody. Generally, the vortex breakdown might be affected by the upstream flow conditions in the pipe. Therefore, it is significant to examine the flows produced by the swirl flow generating equipment. In addition, these might be used as part of the upstream conditions for numerically calculating the swirling flows in the pipe.

According to several experiments, the axial velocity component profile around the upstream cross section of the pipe characteristically has a high velocity near the axis. The circumferential velocity component shows the solid rotation around the pipe axis and the irrotational swirl at the outer region when the Reynolds number is high. Faler and Leibovich[5] represented least square best fit of the experimental data to the profiles $W(r) = W_1 + W_2\exp(-\alpha r^2)$, $V(r) = Kr^{-1}[1-\exp(-\alpha r^2)]$, which correspond to the axial and circumferential velocity components, respectively. W_1, W_2, α, and K are arbitrary constants, and r is the radial location.

The objective of the present Note is to partially explain these characteristics by actually calculating the flow between the bellmouth and centerbody. Although two kinds of effects, large deformation of geometry and viscosity, should be considered, for simplicity we consider only the effect of large deformation and show to what extent the flow can be simulated due to the large deformation. The results are compared with the experimental ones.

Governing Equation

The equations are written in cylindrical coordinates (r,θ,z), where u, v, and w are the velocity components in the r, θ, and z directions, respectively, as shown in Fig. 1. For axisymmetric inviscid swirling flows, the basic equation is written as follows[4]:

$$\frac{\partial^2\psi}{\partial r^2} - \frac{1}{r}\frac{\partial\psi}{\partial r} + \frac{\partial^2\psi}{\partial z^2} + K\frac{dK}{d\psi} - r^2\frac{dE}{d\psi} = 0 \qquad (1)$$

where ψ represents the stream function, $K(\psi)$ the circulation function defined by $K = vr$, and $E(\psi)$ the total energy per mass. The variables are nondimensionalized by the following quantities: r, z, the pipe radius R; u, v, w, the pipe mean velocity Wm; ψ, Wm^2R; E, Wm^2; and K, WmR.

Boundary conditions were treated in the following manner.

Received May 29, 1981; revision received Sept. 8, 1981.

*Research Associate, Dept. of Aeronautical Engineering, present address, NRC Research Associate, NASA Ames Research Center. Member AIAA.

†Graduate Student.

‡Professor, Department of Aeronautical Engineering.

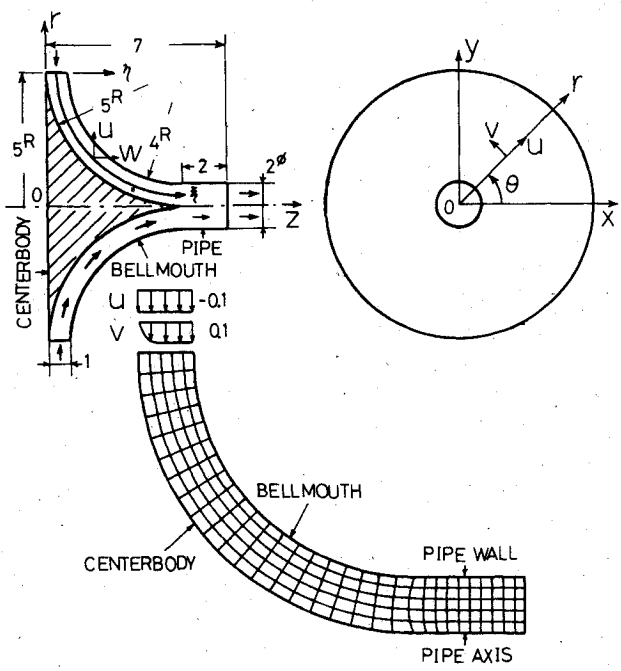

Fig. 1 Region for calculation composing of bellmouth, centerbody, and pipe; and the cylindrical and transformed curvilinear coordinates.

At the inflow section $r=5$, $0\le z\le 1$, and the three velocity components were specified as

$$u=-0.1, \quad v=0.1\ [1-\exp(-10z)], \quad w=0 \tag{2}$$

These expressions are rewritten using ψ and K as follows:

$$\psi=-0.5z, \quad K=0.5\ [1-\exp(20\psi)] \tag{3}$$

At the outflow section $0\le r\le 1$, $z=7$, and the condition that $\partial v/\partial z=0$ was employed, so that $\partial^2\psi/\partial z^2=0$.

The total energy is expressed by K from Eq. (2) as $E=K^2/50+C$, where C is constant. Accordingly, the terms in terms of K and E included in Eq. (1) are arranged as

$$K\frac{dK}{d\psi}-r^2\frac{dE}{d\psi}=\left(\frac{1-r^2}{25}\right)K\frac{dK}{d\psi} \tag{4}$$

Substituting Eq. (4) into Eq. (1) using Eq. (3), the governing equation to be solved is as follows:

$$\frac{\partial^2\psi}{\partial r^2}-\frac{1}{r}\frac{\partial\psi}{\partial r}+\frac{\partial^2\psi}{\partial z^2}=F(r,\psi) \tag{5}$$

where $F=-5(1-r^2/25)\exp(-20\psi)\ [1-\exp(-20\psi)]$. Here, F/r is the circumferential component of vorticity.

To solve Eq. (5), the boundary-fitted coordinate system approach[7] was used, so that the system was rewritten in the ξ, η coordinates. The generated grid in the physical plane is shown in Fig. 1. The grid does not show the orthogonality around the joint between the swirl generating equipment and the pipe due to the irregularity of the boundary conditions. This transformed system was solved using the point SOR method.

Results and Discussion

Figures 2a and 2b show the axial and circumferential velocity component profiles, respectively. As evident from

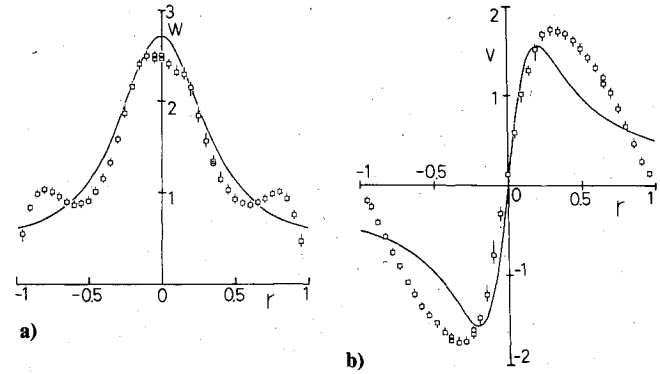

Fig. 2 Calculated results and comparison with experimental data: —, calculated result; ⊏, experimental data[8] with *Re* of 2300 and vane angles of 42 deg at a station located one and seven-eighths times the pipe radius downstream of the upstream end of the pipe; a) axial velocity component and b) circumferential velocity components.

Fig. 2a, the calculated axial velocity profile has a high velocity around the pipe axis. The circumferential velocity component shows the solid rotation around the pipe axis and the irrotation-like swirl at the radial location away from the axis. Part of the experimental results obtained by one of the authors and colleagues[8] is also shown by the symbol ⊏ in these figures for comparison. This experiment was performed under the conditions of the vane angles of 42 deg and a Reynolds number of 2300. In the present calculation, the magnitudes of the radial velocity and the circumferential velocity at the inlet section become equal except near the centerbody, which ideally correspond to the vane angles of 45 deg.

As for the axial velocity component, within half of the pipe radius, the comparison is good, while it is not good in the outer region. This might be due to the lack of viscosity. The circumferential velocity component does not show good agreement except near the axis. The calculated result has smaller core size and circulation than the experimental one. Besides these, a discrepancy arises around the wall. This also is considered to be due to the lack of viscosity and the conditions at the inlet section. Therefore, as the Reynolds number becomes higher, the more similar profiles could be simulated by this calculation method, adjusting the conditions at the inlet section.

References

[1] Harvey, J. K., "Some Observation of the Vortex Breakdown Phenomenon," *Journal of Fluid Mechanics*, Vol. 14, Pt. 4, Dec. 1962, pp. 585-592.

[2] Sarpkaya, T., "On Stationary and Travelling Vortex Breakdowns," *Journal of Fluid Mechanics*, Vol. 45, Pt. 3, Feb. 1971, pp. 545-559.

[3] Sarpkaya, T., "Vortex Breakdown in Swirling Conical Flows," *AIAA Journal*, Vol. 9, Sept. 1971, pp. 1792-1799.

[4] Sarpkaya, T., "Effect of the Adverse Pressure Gradient on Vortex Breakdown," *AIAA Journal*, Vol. 12, May 1974, pp. 602-607.

[5] Faler, J. H. and Leibovich, S., "Disrupted States of Vortex Flow and Vortex Breakdown," *The Physics of Fluids*, Vol. 20, July 1977, pp. 1385-1399.

[6] Faler, J. H. and Leibovich, S., "An Experimental Map of the Internal Structure of a Vortex Breakdown," *Journal of Fluid Mechanics*, Vol. 86, Pt. 2, May 1978, pp. 313-335.

[7] Thompson, J. F., Thames, F. C., and Mastin, C. M., "Automatic Numerical Generation of Body Fitted Curvilinear Coordinate System for a Field Containing Any Number of Arbitrary Two-Dimensional Bodies," *Journal of Computational Physics*, Vol. 15, July 1974, pp. 299-319.

[8] Uchida, S., Nakamura, Y., and Ohsawa, M., "On the Structure of Vortex Breakdown," *Proceedings of the 11th Fluid Dynamic Conference*, Japanese Society of Aerospace Sciences and Japanese Society of Fluid Mechanics, Oct. 1979, pp. 54-57.